

# Hellmann-Feynman theorem and correlation-fluctuation analysis for the Calogero-Sutherland model

Rudolf A Römer<sup>‡</sup>

Institut für Physik, Technische Universität, D-09107 Chemnitz, Germany

Paul Ziesche

Max-Planck-Institut für Physik komplexer Systeme, Nöthnitzer Str. 38, D-01187 Dresden, Germany

**Abstract.** Exploiting the results of the exact solution for the ground state of the one-dimensional spinless quantum gas of Fermions and impenetrable Bosons with the  $\mu/x_{ij}^2$  particle-particle interaction, the Hellmann-Feynman theorem yields mutually compensating divergences of both the kinetic and the interaction energy in the limiting case  $\mu \rightarrow -1/4$ . These divergences result from the peculiar behavior of both the momentum distribution (for large momenta) and the pair density (for small inter-particle separation). The available analytical pair densities for  $\mu = -1/4$ , 0, and 2 allow to analyze particle-number fluctuations. They are suppressed by repulsive interaction ( $\mu > 0$ ), enhanced by attraction ( $\mu < 0$ ), and may therefore measure the kind and strength of correlation. Other recently proposed purely quantum-kinematical measures of the correlation strength arise from the small-separation behavior of the pair density or — for Fermions — from the non-idempotency of the momentum distribution and its large-momenta behavior. They are compared with each other and with reference-free, short-range correlation-measuring ratios of the kinetic and potential energies.

PACS numbers: 71.10.-w, 05.40.-a, 71.45.Gm, 71.10.Hf, 71.10.Pm

Submitted to: *J. Phys. A: Math. Gen.*

<sup>‡</sup> r.roemer@physik.tu-chemnitz.de

## 1. Introduction

In the ground state of electron systems, it has been shown that exchange (X) due to the Pauli ‘repulsion’ and correlation (C) due to the Coulomb repulsion suppress particle-number fluctuations and consequently reduce the energy [1–3]. This energy reduction provides most of the ‘glue’ that binds atoms together to form molecules and solids [4]. Particle-number fluctuations mean that the particle number in a domain (which may be a muffin-tin sphere, a Wigner-Seitz cell, a Bader basin [5], a Daudel loge [6], a bond region between atoms in a molecule, etc.) fluctuates due to zero temperature quantum motion with a certain probability. Fulde [1] takes  $C_2H_2$  as an example for such fluctuations. The number of valence electrons in a sphere containing a C atom fluctuates around its average value  $\approx 3.9$ . Comparison of Hartree-Fock (HF) calculations for  $C_2H_2$  with calculations which include correlation shows that configurations with large deviations from the average valence electron number (e.g., with 0 and 1 or 7 and 8 electrons) are strongly suppressed due to correlation. A similar fluctuation-correlation analysis is performed in Ref. [2] for several dimers and in Ref. [3] for the uniform electron gas in one, two, and three dimensions (1D, 2D, 3D). These calculations for the above mentioned narrowing of the particle-number distribution need the pair density (PD)  $n(\vec{r}_1, \vec{r}_2)$  and this narrowing is used to derive from the PD a quantum-kinematical measure for the correlation strength [1]. Correlation and its strength is furthermore characterized by the small-separation (or on-top) behavior of the PD. The spherically averaged on-top curvature of the spin-parallel PD may serve as a local correlation measure [7] and from the topological analysis of the intracule PD a short-range correlation strength is defined [8]. In addition to these PD based quantities the concept of a correlation ‘entropy’ has been developed for Fermi systems [9–12] (in Ref. [11] the term Jaynes entropy is used). It is based on the correlation induced non-idempotency of the correlated one-particle density matrix (1PDM)  $\gamma(\vec{r}; \vec{r}')$ . All these correlation measures intend to make the qualitative terms ‘weak and strong correlation’ quantitatively precise [13]. Note that strong correlation means extreme narrowing of the particle-number distribution which is usually described as electron localization.

In the present paper, we apply the above mentioned fluctuation-correlation analysis to the exactly solvable Calogero-Sutherland (CS) model [14]. The CS model is a model of long-range-interacting spinless particles in 1D and has been solved exactly by means of the (asymptotic) Bethe-Ansatz technique [14, 15]. The solution is valid for both fermionic and bosonic particle symmetry. Here we will mostly concentrate on the Fermi systems. Furthermore, the model can be shown to be the universal quantum model underlying the dynamical interpretation of random matrix theory [16, 17]. This latter connection has been used to also compute several correlation functions exactly at three special values of the interaction strength, among them the 1PDM and the PD [14]. Thus although the information is restricted to the 1D case, the model nevertheless is ideally suited for testing the fluctuation-correlation measures discussed above.

Correlated 1PDM and correlated PD need correlated many-body wave functions

(beyond the HF caricature), which in quantum chemistry [18, 19] are traditionally obtained from configuration interaction (CI), coupled cluster (CC), Møller-Plesset, quantum Monte Carlo calculations or recently from the contracted-Schrödinger-equation method [20] or the incremental method [21]. All these procedures involve certain approximations or have restricted applicability. So the existence of non-trivial *exactly solvable models* which can provide 1PDM and PD is of much interest for the mentioned fluctuation and correlation analysis.

We shall only consider the ground state properties of the CS model [14]. The interaction is pairwise inversely proportional to the square of the distance  $x_{ij} = |x_i - x_j|$  of two particles with interaction strength  $\mu$ , *i.e.*,  $\mu/x_{ij}^2$ . The interaction strength  $\mu \geq -1/4$  is occasionally parametrized as  $\mu = \lambda(\lambda - 1)$  with a parameter  $\lambda = 1/2 + \sqrt{1/4 + \mu} \geq 1/2$ . We shall mostly use the parameterization  $\nu = \sqrt{1/4 + \mu}$ , such that  $\mu = \nu^2 - 1/4$  and  $\lambda = 1/2 + \nu$ . In the thermodynamic limit we assume constant density  $\rho(x) = n$ , so the CS-ground state has only two parameters,  $\nu$  and  $n$ . The  $1/x_{ij}^2$  interaction has the peculiarity not to possess a natural length. Therefore it is a model showing critical behavior, which can be discussed in terms of universality classes and their conformal anomalies [22–25]. This beauty of the  $1/x_{ij}^2$  interaction shows up also in the analytical Bethe-Ansatz solutions [14, 26–30] and the explicit knowledge of the correlated many-body wave functions [14, 31]. From the Bethe-Ansatz technique the complete energy spectrum and in particular the ground state energy per particle as a function of the interaction strength parameter  $\nu$  is available [14]. We show that its kinetic and interaction ‘components’ can be deduced with the help of the Hellmann-Feynman theorem [32]. Surprisingly, when the interaction strength parameter  $\nu$  approaches its limiting value 0, both the kinetic and the interaction energy diverge in such a way that they compensate each other leaving the total energy finite. As we outline in the following, these divergences result from the peculiar behavior of the 1PDM and the PD for  $\nu \rightarrow 0$  and are related to the “fall-into-the-origin” already mentioned in Ref. [33].

For  $\nu = 0, 1/2$ , and  $3/2$  — corresponding to  $\mu = -1/4, 0$  and  $2$  or  $\lambda = 1/2, 1$ , and  $2$  — it has been shown [14] that the square of the ground state wave function is intimately related to the eigenvalue distribution of random matrices of the orthogonal ensemble, the unitary ensemble, and the symplectic ensemble, respectively. Using this connection, Sutherland had shown how to construct the 1PDM and the PD using integral relations of random matrix theory. The resulting formulas reduce the problem, say for the 1PDM, from the evaluation of a high-dimensional integral to the computation of a determinant of a matrix [15]. From the 1PDM  $\gamma(x - x')$ , the momentum distributions  $n_\kappa$  for the three special values of  $\nu$  follow via Fourier transform. Due to correlation the latter quantities are non-idempotent. They determine the mentioned correlation entropy per particle  $s = -\sum_\kappa n_\kappa \ln n_\kappa / \sum_\kappa n_\kappa$ . Knowledge of the PD  $n(x_{12})$  allows [14, 15, 34, 45] us to calculate the fluctuation  $\Delta N_X$  of the particle-number around its mean value  $N_X = nX$  in any piece (domain)  $X$  of the  $x$ -axis. Comparing this variance of the particle-number distribution  $P_X(N)$  for the cases ‘no correlation’ ( $\nu = 1/2$  or HF approximation) and ‘correlation’ shows the above mentioned narrowing for repulsion ( $\nu > 1/2$ ) in a smaller

$\Delta N_X$ . Contrarily, for attraction ( $\nu < 1/2$ ) a broadening with a larger  $\Delta N_X$  appears.

In Section 2, we introduce the CS model, define the kinematical quantities used throughout the text, and present the Hellmann-Feynman theorem. Section 3 is devoted to the thermodynamic limit. In Section 4, after presenting the HF approximation, we discuss first qualitatively and then analytically the influences of the CS interaction on 1PDM and PD. In particular, we show that the above mentioned divergences in kinetic and potential energies are caused by a peculiar behavior of the PD  $n(x_{ij})$  for *small inter-particle separations*  $x_{ij} \ll k_F^{-1}$  and of the momentum distribution  $n_\kappa$  for *large momenta*  $k \gg k_F$  or  $\kappa \equiv k/k_F \gg 1$ . In Section 5 we then apply the mentioned fluctuation-correlation measures to the CS model. Section 6 is devoted to details of the numerics and in Section 7 we discuss extensions of our approach to impenetrable Bosons and lattice gases. We conclude in Section 8 with a discussion of our results.

## 2. The system and its ground state

### 2.1. Hamiltonian, energies, and quantum kinematical quantities

The Hamiltonian of the CS model is  $\hat{H} = \hat{T} + \hat{V}$  with

$$\hat{T} = \sum_i^N \frac{1}{2} p_i^2 \quad , \quad \hat{V} = \sum_i^N v_{\text{ext}}(x_i) + \sum_{i < j}^N \frac{\nu^2 - \frac{1}{4}}{x_{ij}^2} \quad , \quad (2.1)$$

with  $p_i^2 = -\partial^2/\partial x_i^2$ , and  $N$  equal to the number of particles. We assume the system to be confined to the length  $L$  by an external potential  $v_{\text{ext}}(x)$ , *e.g.*, a box or harmonic oscillator potential. In the following we alternatively assume periodic boundary conditions with  $v_{\text{ext}}(x) = 0$  and a density in the  $k$  space described by  $L\Delta k/(2\pi) = 1$  [14,35]. The average particle density is  $n = N/L$ . Furthermore, it follows from dimensional reasons that all energies for the Hamiltonian (2.1) are proportional to  $n^2$  in agreement with the virial theorem and all lengths are measured in units of  $1/n$  (thus  $k_F \sim n$ ) [14].

We denote the ground state energy and its kinetic and potential ‘components’ by  $E_N = \langle \hat{H} \rangle$ ,  $T_N = \langle \hat{T} \rangle$ , and  $V_N = \langle \hat{V} \rangle$ , respectively. Then the corresponding energies per particle are  $e_N = E_N/N$ ,  $t_N = T_N/N$ ,  $v_N = V_N/N$  with  $e_N = t_N + v_N$ . From the antisymmetric (or symmetric) ground state wave function follow by contractions [14,15] the 1PDM  $\gamma_N(x; x')$  and the PD  $n_N(x_1, x_2)$  normalized as  $\int dx \gamma_N(x; x) = N$  and  $\int dx_1 \int dx_2 n_N(x_1, x_2) = N(N-1)$ , respectively. The PD describes the XC hole, vanishing for zero separation and approaching the Hartree product  $\rho_N(x_1)\rho_N(x_2)$  for large separations. The cumulant PD  $w_N(x_1, x_2) \equiv \rho_N(x_1)\rho_N(x_2) - n_N(x_1, x_2)$  is via

$$\int dx_1 \int dx_2 w_N(x_1, x_2) = N \quad (2.2)$$

size-extensively normalized. Furthermore with the abbreviation  $y = k_F x$ ,  $k_F = \pi n$  [14], and with the *dimensionless functions*  $f_N(y_1; y_2)$  hermitian,  $g_N(y_1, y_2)$  non-negative, and  $h_N(y_1, y_2) \equiv f_N(y_1; y_1)f_N(y_2; y_2) - g_N(y_1, y_2)$ , we can write for the 1PDM  $\gamma_N(x_1; x_2) =$

$n f_N(y_1; y_2)$ , for the PD  $n_N(x_1, x_2) = n^2 g_N(y_1, y_2)$ , and for the cumulant PD we have  $w_N(x_1, x_2) = n^2 h_N(y_1, y_2)$ . The dimensionless cumulant PD is thus  $h_N = 1 - g_N$  and normalized as

$$\frac{1}{N} \int \frac{dy_1}{\pi} \frac{dy_2}{\pi} h_N(y_1, y_2) = 1, \quad (2.3)$$

which follows from Equation (2.2). With these dimensionless 1PDM and PD and with the Fermi energy  $\epsilon_F = k_F^2/2$  the energies  $t_N$  and  $v_N$  are given by

$$t_N = \frac{1}{N} \int \frac{dy_1}{\pi} \left[ -\frac{\partial^2}{\partial y_1^2} f_N(y_1; y_2) \right]_{y_2=y_1} \epsilon_F \quad (2.4a)$$

and

$$v_N = \frac{1}{N} \int \frac{dy_1}{\pi} \frac{dy_2}{\pi} g_N(y_1, y_2) \frac{\mu}{y_{12}^2} \epsilon_F. \quad (2.4b)$$

Therefore  $t_N/\epsilon_F$ ,  $v_N/\epsilon_F$  and  $e_N/\epsilon_F$  are functions of  $\mu$  and  $N$ . The latter dependence disappears for the thermodynamic limit as shown in Section 3.

## 2.2. The Hellmann-Feynman theorem

If  $e_N$  is known as a function of  $\mu$ , then  $t_N$  and  $v_N$  can be obtained from the Hellmann-Feynman theorem [32] without knowing the quantum-kinematical quantities  $f_N(y_1; y_2)$  and  $g_N(y_1, y_2)$ . This theorem says

$$\frac{\partial E_N}{\partial \mu} = \left\langle \frac{\partial \hat{H}}{\partial \mu} \right\rangle \quad (2.5)$$

which for (2.1) gives

$$v_N = \mu \frac{\partial e_N}{\partial \mu}, \quad t_N = \left( 1 - \mu \frac{\partial}{\partial \mu} \right) e_N \quad (2.6)$$

and also

$$\frac{\partial}{\partial \mu} t_N = -\mu \frac{\partial}{\partial \mu} \left( \frac{1}{\mu} v_N \right). \quad (2.7)$$

Thus — with Equation (2.1) in mind — the Hellmann-Feynman relation (2.5) for the  $1/x_{ij}^2$  model establishes an integral relation between the dimensionless 1PDM  $f_N$  on the l.h.s. and the dimensionless PD  $g_N$  on the r.h.s. of Equation (2.7).

## 3. Thermodynamic limit

We wish to study the thermodynamic limit with  $N \rightarrow \infty$  and  $L \rightarrow \infty$  such that  $n = N/L = \text{const.}$  The resulting extended system has only two parameters, the interaction strength parameter  $\nu$  and the Fermi wave number  $k_F$ . So  $t/\epsilon_F$ ,  $v/\epsilon_F$ , and  $e/\epsilon_F$  become functions of  $\nu$  only. The thermodynamic limit makes furthermore the 1PDM and the PD to depend only on  $k_F x_{12} \equiv k_F(x_1 - x_2) = y_1 - y_2 \equiv y_{12}$ . The dimensionless functions  $f_N$ ,  $g_N$ , and  $h_N$  then take the forms  $f(y_{12})$ ,  $g(y_{12})$ , and  $h(y_{12}) = 1 - g(y_{12})$ ,

respectively, with  $f(0) = 1$  and  $g(0) = 0$  or equivalently  $h(0) = 1$ . These functions have  $\nu$  as the only parameter.

The eigenfunctions (or natural orbitals) of the 1PDM  $\gamma(x_{12}) = nf(y_{12})$  become simply plane waves  $\varphi_k^0(x) = e^{ikx}/L$ , such that

$$\gamma(x_{12}) = n \int_0^\infty d\kappa n_\kappa \cos \kappa |y_{12}| \equiv n f(y_{12}), \quad (3.1)$$

where  $n_\kappa$  is the momentum distribution and  $\kappa = k/k_F$ .

For  $\nu = 1/2$  (ideal spinless 1D Fermi gas) the Pauli principle leads in the reciprocal space to the Fermi ice block  $n_\kappa^0 = \theta(1 - |\kappa|)$  and in the direct space to the ideal X hole  $g^0(y) = 1 - [f^0(y)]^2$  with the dimensionless 1PDM  $f^0(y) = (\sin y)/y$  following from Equation (3.1). The energy per particle is  $e_0 = \epsilon_F/3 = k_F^2/6$ .

In general, with  $\gamma(0) = n$ , the momentum distribution  $n_\kappa$  is normalized as  $\sum_\kappa n_\kappa = N$  or

$$\int_0^\infty d\kappa n_\kappa = 1. \quad (3.2)$$

The kinetic energy per particle is according to Equation (2.4a)

$$t = 6 \int_0^\infty d\kappa n_\kappa \frac{\kappa^2}{2} e_0. \quad (3.3)$$

$n_\kappa$  is a function of  $|\kappa|$  and  $\nu$ , so  $t/e_0$  is a function of  $\nu$  only with  $t = e_0$  for  $\nu = 1/2$ .

The corresponding expressions for the PD  $g(y)$  are according to Equation (2.3)

$$2 \int_0^\infty \frac{dy}{\pi} h(y) = 1, \quad h(y) = 1 - g(y) \quad (3.4)$$

and for the interaction energy per particle according to Equation (2.4b)

$$v = 6 \int_0^\infty \frac{dy}{\pi} g(y) \frac{\nu^2 + \frac{1}{4}}{y^2} e_0. \quad (3.5)$$

$g(y)$  is a function of  $y$  and  $\nu$ , so  $v/e_0$  is a function of  $\nu$  only. With  $t$  and  $v$  follows the integral relation

$$\int_0^\infty d\kappa \frac{\kappa^2}{2} \frac{\partial n_\kappa}{\partial \mu} = - \int_0^\infty \frac{dy}{\pi} \frac{\nu^2 + \frac{1}{4}}{y^2} \frac{\partial g(y)}{\partial \mu} \quad (3.6)$$

as a consequence of the Hellmann-Feynman theorem expressed in Equation (2.7). Correlation via  $\nu \neq 1/2$  deforms the X hole and the Fermi ice block as shown in Figs. 2 and 3 in such a way that Equation (3.6) is maintained.

## 4. Hartree-Fock approximation and correlation beyond it

### 4.1. Hartree-Fock (HF) approximation

The simplest approximation for the quantities  $n_\kappa$ ,  $g(y)$ ,  $t$ , and  $v$  is obtained from the HF approach. The momentum distribution in Equation (3.3) and the PD in Equation (3.5) are to be replaced by their ‘ideal’ expressions  $n_\kappa^0$  and  $g^0(y)$ , respectively. Consequently,

we find  $t_{\text{HF}} = e_0$  and  $v_{\text{HF}} = 2\mu e_0$  and thus  $e_{\text{HF}} = (1+2\mu) e_0$ , as shown in Figure 1. Here the identity (A.5) has been used. The total HF energy  $e_{\text{HF}}$  also obeys the Hellmann-Feynman theorem (2.5) and the virial theorem.

#### 4.2. Qualitative discussion of correlation

Due to correlation the true ground state energy per particle,  $e$ , is below the HF energy  $e_{\text{HF}}$  and the true ground state wave function  $\Phi(\dots)$  is no longer a single Slater determinant. Note that the definition of the term ‘correlation’ needs a reasonable reference state, which is  $\Phi_{\text{HF}}(\dots)$  in our case. So, correlation causes a negative correlation energy  $e_{\text{corr}} = e - e_{\text{HF}} < 0$ , namely through redistributions of  $g^0(y)$  and  $n_{\kappa}^0$  which are shown in Figs. 2 and 3 and described in the following.

As we show in Figure 2, correlation modifies the X hole of the unperturbed PD. Especially the correlation induced changes for small  $y$  are of interest, because the interaction  $1/y^2$  is there largest. The on-top behavior of the uncorrelated X hole ( $\nu = 1/2$  or HF) is described by  $g^0(y) = y^2/3 + \dots$ . In its correlated counterpart with a  $\nu$ -dependent exponent and  $\nu$ -dependent coefficients (see Appendix B)

$$\begin{aligned} g(y) &= Ay^{\alpha} (1 + a_1 y + a_2 y^2 + \dots), \\ \alpha &= 1 + 2\nu, \end{aligned} \tag{4.1}$$

correlation for  $\nu \neq 1/2$  shows up in  $\alpha \neq 2$  and  $A \neq 1/3$ . More precisely, repulsive particle interaction ( $\nu > 1/2$ ) supports the Pauli ‘repulsion’, so the X hole is broadened (through increasing  $\alpha$  and decreasing  $A$ ), but attractive particle interaction ( $\nu < 1/2$ ) fights against (or competes with) the Pauli ‘repulsion’, so the X hole is narrowed (through decreasing  $\alpha$  and increasing  $A$ ) as shown in Figure 2 and Table 1. This X hole narrowing (for  $\nu < 1/2$ ) or broadening (for  $\nu > 1/2$ ) makes

$$6 \int_0^{\infty} \frac{dy}{\pi} \frac{g(y)}{y^2} = 1 + \frac{1}{2\nu} \gtrless 2 \quad \text{for} \quad \nu \gtrless \frac{1}{2}. \tag{4.2}$$

The equation follows from Equation (3.5) together with the Hellmann-Feynman theorem (2.5). Thus  $v < v_{\text{HF}} = 2\mu e_0$  for  $\nu \neq 1/2$  as shown in Figure 1.

As shown in Figure 3, correlation thaws the Fermi ice block  $\theta(1 - |\kappa|)$ . Mathematically, the momentum distribution  $n_{\kappa}$  becomes non-idempotent, physically this means: Correlation excites particles for  $\kappa > 1$  and holes for  $\kappa < 1$ . This increases the kinetic energy independent whether the interaction is attractive ( $\nu < 1/2$ ) or repulsive ( $\nu > 1/2$ ):  $t > t_{\text{HF}}$  as can be seen in Figure 1. We note that  $n_{\kappa}$  has no discontinuity at  $|\kappa| = 1$ . Its value is  $1/2$  and near  $\kappa = 1$  it follows a power law as is typical for all Luttinger liquids with their  $z_F = 0$  [36, 37].

We model the melting of the Fermi ice block analytically with the continuous function

$$\begin{aligned} n_{\kappa} &= \frac{1}{2} + B(1 - \kappa)^{\beta} [1 + b_1^-(1 - \kappa)^{\beta} + b_2^-(1 - \kappa)^{2\beta} + \dots] \\ &\quad \text{for } 0 \leq \kappa \leq 1, \end{aligned} \tag{4.3a}$$

$$n_\kappa = \frac{1}{2} - B(\kappa - 1)^\beta [1 + b_1^+(\kappa - 1)^\beta + b_2^+(\kappa - 1)^{2\beta} + \dots] \\ \text{for } 1 \leq \kappa \leq 2, \quad (4.3b)$$

$$n_\kappa = \frac{C}{\kappa^\gamma} \left( 1 + \frac{c_2}{\kappa^2} + \frac{c_4}{\kappa^4} + \dots \right) \\ \text{for } 2 \leq \kappa \leq \infty \quad (4.3c)$$

with [15, 38]

$$\beta = \frac{1}{4} \frac{(1 - 2\nu)^2}{1 + 2\nu} \quad (4.4)$$

and  $\gamma = 3 + 2\nu$  (Appendix B). The exponents  $\beta, \gamma$  and the coefficients  $B, C$ , and  $b_i^\pm, c_i$  depend on  $\nu$ . The condition  $0 < \beta < 1$  ensures an infinite slope of  $n_\kappa$  at  $\kappa = 1$ . This  $n_\kappa$  has to obey the normalization (3.2) and the condition

$$3 \int_0^\infty d\kappa n_\kappa \kappa^2 = \frac{\left(\frac{1}{2} + \nu\right)^2}{2\nu} \geq 1, \quad (4.5)$$

which follows from Equation (3.3) together with the Hellmann-Feynman theorem (2.5). For  $\nu = 1/2$  (or HF) it is  $\beta = 0$ ,  $B(1 + \sum_i b_i^\pm) = \frac{1}{2}$ , and  $C = 0$ . The correlation induced melting for  $\nu \neq 1/2$  shows up in  $\beta > 0$ ,  $B(1 + \sum_i b_i^\pm) < \frac{1}{2}$ , and  $C > 0$ .

#### 4.3. Results of the exact solution

With the help of the Bethe-Ansatz technique one obtains  $e = \lambda^2 e_0$  [14, 15].  $e$  as a function of the interaction strength parameter  $\lambda$  shows no special behavior for  $\lambda \xrightarrow{>} 1/2$ , but as a function of the interaction strength  $\mu = \lambda(\lambda - 1)$ ,

$$e = \left(\frac{1}{2} + \nu\right)^2 e_0, \quad \nu = \sqrt{\frac{1}{4} + \mu} \quad (4.6)$$

the non-analytical behavior for  $\mu \rightarrow -1/4$  is incorporated in the variable  $\nu$ .

Equation (4.6) yields with the Hellmann-Feynman theorem (2.6) the kinetic energy per particle,

$$t = \frac{\left(\frac{1}{2} + \nu\right)^2}{2\nu} e_0. \quad (4.7)$$

Equation (4.6) yields with Equation (2.6) also the interaction energy per particle

$$v = \mu \left( 1 + \frac{1}{2\nu} \right) e_0. \quad (4.8)$$

From Figure 1 we see that both  $t$  and  $v$  diverge for  $\nu \rightarrow 0$ , while  $e$  remains finite.

Equations (4.7) and (4.8) lead to

$$\int_0^\infty d\kappa n_\kappa \kappa^2 = 6\nu \left[ \int_0^\infty \frac{dy}{\pi} \frac{g(y)}{y^2} \right]^2, \quad (4.9)$$

as another integral relation between the momentum distribution  $n_\kappa$  and the dimensionless PD  $g(y)$  in addition to Equation (3.6). These distribution functions have

to change with  $\nu$  in such a way that these relations (3.6) and (4.9) are obeyed together with the normalization conditions (3.2) and (3.4).

The PD  $n(x_{12}) = n^2 g(y)$  with  $y = k_F x_{12}$  is known analytically for the values  $\nu = 0, 1/2$ , and  $3/2$  [14, 15]. For  $\nu = 0$  it is (with the notation of Appendix A)

$$g(y) = 1 - \left( \frac{\sin y}{y} \right)^2 + \text{Si}(y) \frac{d}{dy} \frac{\sin y}{y} - \frac{\pi}{2} \frac{d}{dy} \frac{\sin y}{y}, \quad (4.10)$$

for  $\nu = 1/2$  (ideal Fermi gas) it is

$$g(y) = 1 - \left( \frac{\sin y}{y} \right)^2, \quad (4.11)$$

and for  $\nu = 3/2$  it is

$$g(y) = 1 - \left( \frac{\sin 2y}{2y} \right)^2 + \text{Si}(2y) \frac{d}{d(2y)} \frac{\sin 2y}{2y}. \quad (4.12)$$

The corresponding dimensionless cumulant PDs  $h(y) = 1 - g(y)$  are given in Table 2 together with their Fourier transforms

$$\tilde{h}(q) = 2 \int_0^\infty dy \cos(qy) h(y). \quad (4.13)$$

They have via  $S(q) = 1 - \tilde{h}(q)/\pi$  a simple relation to the static structure factor (or van Hove correlation function)  $S(q) = \langle \hat{\rho}_q \hat{\rho}_q^\dagger \rangle / N$ , which describes the correlation of density-density fluctuations.  $\hat{\rho}_q = \sum_i \exp(-iqx_i)$  is the Fourier transform of the density operator  $\hat{\rho}(x) = \sum_i \delta(x - x_i)$ . The three PDs  $g(y)$  are shown in Figure 2 and the three structure factors  $S(q)$  in Figure 4.

For  $\nu = 1/2$  the weak oscillations of  $g(y)$  and the (first-order) kink of  $S(q)$  arise from the Fermi momentum distribution  $n_\kappa$  with its sharp discontinuity  $z_F = 1$  at  $\kappa = 1$ . With increasing repulsion the oscillations of  $g(y)$  are enhanced, what is displayed in the reciprocal space by the peak of  $S(q)$  at  $q = 2$  (and a 3rd-order kink at  $q = 4$ ). This peak is customary in 1D quantum liquids, see, e.g., the spin-correlation functions of Ref. [39]. The first maximum of  $g(y)$  runs through a certain trajectory from  $(\pi, 1)$  to  $(2.99, 1.24)$ . Whereas repulsion enhances the Friedel oscillations of  $g(y)$  and the kink structure of  $S(q)$ , they diminish with increasing attraction: for  $\nu = 0$  both  $g(y)$  and  $S(q)$  approach the value 1 smoothly (non-oscillatory) from below. The discontinuity for  $\nu = 0$  of the second derivative of  $S(q)$  at  $q = 2$  replaces the kink seen for other values of  $\nu$ . For the on-top behavior of  $g(y)$  in terms of  $g(0)$ ,  $g'(0)$ ,  $g''(0)$  the following holds: It is  $g(0) = 0$ , according to the Pauli principle,  $g'(0) = \pi/6$  for  $\nu = 0$ , but 0 for  $\nu > 0$ , and it is  $g''(0) = 0$  for  $\nu = 0$ , infinite for  $0 < \nu < 1/2$ , but  $2/3$  for  $\nu = 1/2$ , and 0 for  $\nu > 1/2$ . We remark that  $S(q)$  and  $g(y)$  can be computed also for other values of  $\nu$  in addition to the three special values used here [34, 45].

With the identities (A.2)–(A.4) the normalization condition (3.4) is fulfilled. From Equations (4.10)–(4.12) follow the on-top coefficients of Equation (4.1); they are shown in Table 1. Note that the last two terms of Equation (4.10) do not contribute to the normalization because of Equation (A.3) and that the last term causes the odd on-top

coefficients of Table 1 and also the linear behavior for small  $y$ . Its oscillations are exactly canceled by the combined oscillations of the second and the third term. Simultaneously, these terms ensure the correct normalization.

The PD (4.11) for  $\nu \rightarrow 1/2$  plugged into Equation (2.4b) yields with the identity (A.5) the same as results from Equation (4.8), which follows from the total energy per particle, Equation (4.6), and the Hellmann-Feynman theorem (2.6), namely  $v = 2\mu e_0$ . Similarly the PD (4.12) for  $\nu \rightarrow 3/2$  plugged into Equation (3.5) yields with the identities (A.5) and (A.6) the same as results from Equation (4.8)), namely  $v = 4\mu e_0/3$ .

For  $\nu = 0$  a divergence appears, because from the PD (4.10) follows an on-top behavior, which is linear in  $y$  as shown in Figure 2 and Table 1. This linear behavior results from the last term of Equation (4.10), which does not influence the normalization (3.4), but it makes the interaction energy  $v \sim \int_0^\infty dy g(y)/y^2$  to diverge logarithmically in agreement with the divergence of  $v \rightarrow -e_0/8\nu$  for  $\nu \rightarrow 0$  as displayed in Figure 1.

The divergence of the interaction energy is accompanied and compensated by the corresponding divergence of the kinetic energy  $t \rightarrow e_0/8\nu$ . This indicates a special asymptotic behavior of the momentum distribution  $n_\kappa$  for  $\nu \rightarrow 0$ , namely Equation (4.3c) with  $\gamma \rightarrow 3$ . For  $\gamma > 3$  the integral  $\int_0^\infty d\kappa n_\kappa \kappa^2$  is convergent, but with  $\gamma \rightarrow 3$  for  $\nu \rightarrow 0$  it diverges logarithmically, whereas the normalization integral (3.2) remains convergent. The counterpart to this asymptotic behavior of  $n_\kappa$  for  $\kappa \rightarrow \infty$  is the on-top behavior of the PD for  $y \rightarrow 0$  as shown in Figure 2 and Table 1 with a smooth transition of the coefficient  $A$  in Equation (4.1) from  $\pi/6$  via  $1/3$ , to  $16/135$  for  $\nu = 0$ ,  $1/2$  and  $3/2$ , respectively. With quadratic interpolation of the coefficients shown in Table 1 as functions of  $\nu$ , one may continuously switch the on-top behavior of the PD  $g(y)$  between its forms at  $\nu = 0$  and  $3/2$ . For the PD exponent  $\alpha = 1 + 2\nu$  we refer to Appendix B, where also the momentum-distribution exponent is conjectured as  $\gamma = 3 + 2\nu$ .

These divergences of the kinetic and the interaction energies indicate that for attractive particle interaction  $\mu/x_{ij}^2$  with  $\mu \rightarrow -1/4$  the system becomes unstable (no ground state with finite kinetic and potential energies). We remark that it was shown in Ref. [33] that the singular particle interaction  $-|\mu|/|\vec{r}_{12}|^2$  makes already two particles to fall together (“fall-into-the-origin”) for  $|\mu| > 1/4$  (ground state with  $E \rightarrow -\infty$ ) and for  $|\mu| < 1/4$  there are only scattering states with  $E \geq 0$  (no bound states with  $E < 0$ ) [14].

For  $\nu = 0$  the exact solution of the CS model yields the momentum-distribution data. In Section 6 we will give the details of the necessary numerical calculation. The coefficients of Equation (4.3a) are fitted to the  $n_\kappa$  values for  $\kappa = 0 \dots 1$  and the coefficients of Equation (4.3b) are fitted to the  $n_\kappa$  values for  $\kappa = 1 \dots 2$ . The coefficients are chosen to make also  $n_\kappa$  at  $\kappa = 2$  continuous and smooth. Finally  $b_3^+$  is fine tuned to make the normalization equal to 1 according to (3.2). The results are shown in Figure 3 and the values of the coefficients are given in Table 3. The case  $\nu = 3/2$  is similarly treated only with the difference that also the kinetic energy  $t = \frac{4}{3}e_0$  can be used for the fine tuning in addition to the normalization condition (3.2). The results are shown also in Table 3. Here  $b_3^+$  and  $b_4^+$  have been used for fine tuning (which yields the normalization 0.997 and  $t = 1.34 e_0$ , instead of 1 and  $4e_0/3$ ).

## 5. Fluctuation-correlation analysis

### 5.1. Quantities following from the pair density

*Particle-number fluctuations:* Following Fulde [1] one may ask to what extent correlation influences particle-number fluctuations  $\Delta N_X$  in a domain  $X$ , *i.e.*, a certain interval of the  $x$  axis, where in the average there are  $N_X = nX$  particles. These fluctuations are measured quantitatively by [1, 3, 13]

$$\begin{aligned} \frac{(\Delta N_X)^2}{N_X} &= 1 - \frac{1}{nX} \int_0^X dx_1 \int_0^X dx_2 w(x_{12}) \\ &= 1 - \frac{1}{Y} \int_0^Y dy_1 \int_0^Y dy_2 \frac{h(y_{12})}{\pi}, \end{aligned} \quad (5.1)$$

with  $Y = k_F X = \pi nX$ . Following the Appendix A of Ref. [3] the 2D integral (5.1) is reduced to a 1D integral with the help of the Fourier transform (4.13), namely

$$\frac{(\Delta N_X)^2}{N_X} = 1 - \frac{2}{Y} \int_0^\infty \frac{dq}{\pi} \frac{1 - \cos(qY)}{q^2} \frac{\tilde{h}(q)}{\pi}. \quad (5.2)$$

The results are shown in Figure 5, where also the case  $\nu \rightarrow \infty$  ('strict' or 'perfect' correlation) [3] is displayed. Traces of the oscillations as  $\nu \rightarrow \infty$  are already visible for  $\nu = 3/2$ .

With  $h(y) = 1 - g(y)$  and with the expansion of  $g(y)$  according to Equation (4.1) — see also the text after Equation (4.12) — the small- $X$  expansion of Equation (5.1) is

$$\begin{aligned} \frac{(\Delta N_X)^2}{N_X} &= 1 + d_1 nX + d_2 (nX)^2 + d_3 (nX)^3 \\ &\quad + d_4 (nX)^4 + d_5 (nX)^5 + \dots \quad . \end{aligned} \quad (5.3)$$

The slope  $d_1$  at  $X = 0$  does not depend on the interaction strength parameter  $\nu$  as shown in Table 4 because of  $g(0) = 0$  and  $h(0) = 1$  not depending on  $\nu$ ; but the coefficients of the next terms do such that the particle-number fluctuations are suppressed due to repulsive particle interaction, but enhanced due to attractive particle interaction: correlation makes the particle-number distribution  $P_X(N)$  more narrow for repulsion ( $\nu > 1/2$ ) and more broad for attraction ( $\nu < 1/2$ ). We remark, that fluctuation enhancement (induced by attractive interaction) generally may support/cause clusterings (*e.g.*, paramagnons prior the para-to-ferromagnetic phase transition). In our case this tendency shows up in the sudden "fall-into-the-origin" at  $\nu = 0$ . If one considers with  $X = 1/n$  a Wigner-Seitz 'sphere' (with 'radius'  $X/2$  and  $N_X = 1$ ), then

$$\Sigma_1(\nu) = 1 - \frac{\chi(\nu)}{\chi(1/2)}, \quad \chi(\nu) = \frac{(\Delta N_X)^2}{N_X} \quad (5.4)$$

is a reasonable correlation measure based on particle-number fluctuations as we show in Figure 6.

*On-top behavior:* The exponent  $\alpha$  and the coefficients  $A, a_i$  of Equation (4.1) describe the short-range or dynamical correlation, *i.e.*, the small-separation behavior of  $g(y)$ , see Table 1. Cioslowski's correlation cage [8] is in our case simply the inter-particle-separation range  $y = 0 \dots y_{\max}$  with  $y_{\max}$  being that separation where the PD  $g(y)$  has its first maximum  $g_{\max} = g(y_{\max})$ . For  $\nu = 0, 1/2, 3/2$  the corresponding values are  $y_{\max} = \infty, \pi, 2.99$  and  $g_{\max} = 1, 1, 1.24$  [3]. One may ask to what extent the correlation cage contributes to the interaction energy and define

$$\Sigma_2(\nu) = 1 - \frac{V_{\text{cage}}(\nu)}{V_{\text{cage}}(1/2)}, V_{\text{cage}}(\nu) = \frac{\int_0^{y_{\max}} dy g(y)/y^2}{\int_0^{\infty} dy g(y)/y^2} \leq 1 \quad (5.5)$$

as an energetic correlation measure with  $V_{\text{cage}}(0) = 1$ ; the expression simplifies when using (4.2). Both  $\Sigma_1$  and  $\Sigma_2$  vanish for  $\nu = 1/2$  as shown in Figure 6.

### 5.2. Quantities following from the momentum distribution

*Critical exponent:* The critical or correlation exponent  $\beta$  of Equation (4.4) can be computed from conformal field theory [15, 38]. It describes (together with the coefficient  $B$ ) the behavior of  $n_{\kappa}$  near  $\kappa = 1$  according to Equations (4.3a) and (4.3b). For the three special values  $\nu = 0, 1/2$  and  $3/2$ , this gives  $1/4, 0$ , and  $1/4$ , respectively, as shown in Figure 6. The exponent  $\gamma$  describes the decay of the correlation tail.

*Non-idempotency and correlation entropy:* The  $q$ th order non-idempotency is [12]  $c(q) = 1 - \int_0^{\infty} d\kappa (n_{\kappa})^q$ . The derivative of  $c(q)$  at  $q = 1$  is  $s \equiv c'(1)$  or

$$s(\nu) = - \int_0^{\infty} d\kappa n_{\kappa} \ln n_{\kappa} \geq 0 \quad (5.6)$$

to be referred to as correlation entropy [12, 13]. It has been plotted in Figure 6.

*Correlation tail properties:* The relative number of particles (or holes) in the corresponding correlation tail is [12, 13, 40]

$$N_{\text{tail}}(\nu) = \int_1^{\infty} d\kappa n_{\kappa} = \int_0^1 d\kappa (1 - n_{\kappa}) < 1. \quad (5.7)$$

The contribution of the correlation tail to  $s$  is [13]

$$S_{\text{tail}}(\nu) = - \int_1^{\infty} d\kappa n_{\kappa} \ln n_{\kappa} < s(\nu). \quad (5.8)$$

In addition to these quantum-kinematic measures one may use [13]

$$T_{\text{tail}}(\nu) = \frac{\int_1^{\infty} d\kappa n_{\kappa} \kappa^2}{\int_0^{\infty} d\kappa n_{\kappa} \kappa^2} \leq 1 \quad (5.9)$$

as another energetic measure with  $T_{\text{tail}}(0) = 1$ . Also these correlation measures vanish for  $\nu = 1/2$  as shown in Figure 6.

### 5.3. The correlation energy

For  $e_{\text{corr}} = e - e_{\text{HF}}$  follows

$$e_{\text{corr}} = - \left( \nu - \frac{1}{2} \right)^2 e_0. \quad (5.10)$$

Kinetic and interaction energy contribute  $t_{\text{corr}} = -\frac{1}{2\nu}e_{\text{corr}}$  and  $v_{\text{corr}} = \left(1 + \frac{1}{2\nu}\right)e_{\text{corr}}$ , respectively, to  $e_{\text{corr}}$ .

### 5.4. Comparison of the correlation measures

When comparing the computed correlation measures in Figs. 6 it turns out that for small  $|\nu - 1/2|$  the PD based measures  $\Sigma_{1,2}$  of Eqs. (5.4) and (5.5) are proportional to  $\nu - 1/2$  (which is  $-e'_{\text{corr}}/(2e_0)$ ), whereas the  $n_{\kappa}$  based measures (5.6)–(5.9) as well as (4.4) behave like  $(\nu - 1/2)^2$  (which is  $-e_{\text{corr}}/e_0$ ). So the latter ones are not so sensitive as the first ones. With  $s(\nu) = 0.5828|e_{\text{corr}}/e_0| + \dots$  the Collins' conjecture  $|e_{\text{corr}}| \sim s$  is confirmed at least for weak interaction. In this limit also  $N_{\text{tail}}$ ,  $S_{\text{tail}}$  and  $T_{\text{tail}}$  are mutually proportional and their derivatives are proportional to  $\Sigma_1$  and  $\Sigma_2$ .

We remark that the quantities  $\chi(\nu)$ ,  $V_{\text{cage}}(\nu)$ ,  $N_{\text{tail}}(\nu)$ ,  $S_{\text{tail}}(\nu)$ , and  $T_{\text{tail}}(\nu)$  are reference free, *i.e.*, they are defined without reference to the non-interacting case  $\nu = 1/2$  — which in our case is simultaneously equivalent to the Hartree-Fock approximation. Reference quantities appear in  $\Sigma_{1,2}$  with  $\chi(1/2)$  and  $V_{\text{cage}}(1/2)$  and in  $s(\nu)$  with  $s(1/2) = 0$ . Whereas this observation is important for quantum chemistry — as stressed by J. Cioslowski [8] — whenever multi configuration appears, it is less important in our case which is well described by single configuration.

## 6. Numerical determination of 1PDM and $n(\kappa)$ for the CS model

Results from the theory of random matrices enable the calculation of various correlation functions for the CS model [14, 15, 28–30]. In particular, the 1PDM can be expressed in terms of a determinant of an appropriate matrix  $F_{pq}^{(\nu)}$  [14, 15]. The size of this matrix is specified by the number of particles  $N$  to be  $(N-1)^2$  for  $\nu = 1/2$  and  $3/2$  and  $(N-1)^2/4$  for  $\nu = 0$ . Each element of  $F_{pq}^{(\nu)}$  contains simple trigonometric 1D ( $\nu = 1/2$  and  $3/2$ ) or 2D ( $\nu = 0$ ) integrals.

For some cases, most notably  $\nu = 1/2$ , the resulting determinant can be computed analytically and corresponding expressions have been given in Ref. [15]. For the other cases, we have evaluated the determinant numerically [15], using a subdivision of the system volume (periodicity length) according to  $L/L_0 = 42, 402$ , and  $402$  for  $\nu = 0$ ,  $1/2$ , and  $3/2$ , respectively. The particle number, odd due to periodicity of the wave function [15], varied from  $N = 1$  to  $401$ , corresponding to a variation in density  $n$  from nearly 0 to nearly 1. Taking the Fourier transform, we next compute the momentum distribution  $n_{\kappa}$  for all densities. In the inset of Figure 3, we show results for one of the three special  $\nu$  values.

Next, we apply the definitions of correlation measures and correlation energies as given in Sections 3, 4, and 5 and study their density dependence. In Figure 7 we show results for the entropy  $s$  and in Figure 8 for the various energies as the density is varied. As *all* energies scale with  $n^2$ , these measures should be *density independent* when normalized with respect to  $e_0$ . However, we do in fact see a pronounced density dependence for  $n \gtrsim 0.5/L_0$  and also for  $n \lesssim 0.05/L_0$ . This latter density dependence is simply due to the small particle numbers, thus a small size of  $F_{pq}^{(\nu)}$  and consequently a limited resolution when computing the 1PDM at fixed  $L/L_0$ . The density dependence at large  $n$  values is more intricate to explain. The computation of the 1PDM by the connection with random matrix theory works for the *periodic* model [35]. Thus there exists a Brillouin zone and the tail of  $n_\kappa$  for  $|\kappa|$  outside this Brillouin zone is folded back into it. The tail of  $n_\kappa$  thus tends to be dominated by this effect for large  $n$  values as shown in the inset of Figure 3. However, knowing that the correlation measures must be independent of density in the thermodynamic limit, we deduce their values by restricting us to these density regions where the independence holds. Then we apply the fit according to Equation (4.2) as explained in Section 4.2. In Figure 6 we indicate by error bars the small variation in the correlation entropy when using instead of  $n_\kappa$  as in Figure 3 the  $n_\kappa$  as in the inset. Similarly, the corresponding variations in  $N_{\text{tail}}$ ,  $S_{\text{tail}}$ , and  $T_{\text{tail}}$  are within the symbol sizes.

## 7. Extension to impenetrable Bosons and lattice gases

As mentioned in the introduction, the CS model is also solvable for bosonic particle symmetry. The bosonic wave functions have to obey an additional boundary condition, namely they have to vanish for inter-particle separations  $x_{ij} \rightarrow 0$  such that the resulting system consists of *impenetrable* or hard-core particles [14] with additional  $\mu/x_{ij}^2$  interaction. Both PD and 1PDM may be calculated as before. The PD is independent of statistics [14], thus the fermionic exchange hole agrees with the bosonic impenetrability hole and all quantities computed before based on the PD are the same in the bosonic and the fermionic case. For the 1PDM this is different, the momentum distribution of Bosons is quite different from the fermionic  $n_\kappa$  as shown in Figure 9. However, energetic quantities and correlation measures based upon those are nevertheless independent of the statistics and should thus be the same for Bosons and Fermions. In Figure 8 we show that this is indeed the case. Thus besides the density independence we have another criteria that allows us to extract the correct values of the correlation measures from these plots. We note that the abovementioned unwanted density dependence is also present in the bosonic  $n_\kappa$  and visible in Figs. 7 and 8. Also present is the aliasing effect as shown in the inset of Figure 9.

In Refs. [14, 15], it had been shown to be useful to restrict the family of wave functions of the CS model for both bosonic and fermionic symmetry to a lattice such that the coordinates are integers  $x_j = 1, 2, \dots, L$  [41–43]. Only the normalization constants of the wave functions change and the 1PDM can be computed much as before [14],

replacing the integrals in  $F_{pq}^{(\nu)}$  by appropriate sums [15]. Furthermore, the structure factor  $S(q)$  is known exactly and therefore also the PD [15]. The resulting lattice gas has a particle-hole symmetry and thus we need to consider  $n \leq 1/2L_0$  only. However, the density  $N/L$  now enters all expressions in a non-trivial way and the very useful density independence of the continuum model for the quantities considered here is no longer applicable. Nevertheless, the continuum model corresponds to the low-density limit of the discrete model. In Figure 7, we show that this is indeed the case for, *e.g.*, the correlation entropy.

## 8. Discussion and Conclusions

Both the PD based and the  $n_\kappa$  based correlation measures (4.4) and (5.4)–(5.9) vanish for  $\nu = 1/2$  (no interaction). But the first ones are more sensitive because of  $\Sigma_{1,2} \sim \nu - 1/2$  near to the no-interaction point as shown in Figure 6 (c), while the second ones are  $\sim (\nu - 1/2)^2$  like  $e_{\text{corr}}$  of Equation (5.10) as shown in Figs. 6 (a) and (b) and therefore cannot distinguish between attractive and repulsive interactions. In 1D the PD based measures (5.4) and (5.5) are identical for fermionic and (hard core) bosonic particles. The  $n_\kappa$  based measures (4.4) and (5.6)–(5.9) do not apply for bosonic particles, they are designed for fermionic particles only and appropriate bosonic variants still have to be defined.

For repulsive particle interaction results well-known from other extended many-body systems, such as enhancement of the Friedel oscillations with maxima/minima trajectories (Figure 2), humps/peaks of the static structure factor developing from its non-interacting kink (Figure 4), suppression of particle-number fluctuations (Figure 5), are confirmed again. However, for attractive interactions, we have found in the present work that particle-number fluctuations are *contrarily enhanced* and that this is accompanied by a smoothening of the PD (the oscillations disappear) and of the static structure factor (the kink disappears) as well as by the appearance of a linear on-top behavior of the PD. The latter behavior results in a diverging interaction energy in the strong attraction limit although the total energy remains finite. In momentum space the Fermi ice block thaws for both cases and correlation tails develop. In the strong attraction limit the correlation tail becomes so long ranged that the kinetic energy diverges, thereby exactly compensating the divergence of the interaction energy. We have shown that these divergences can be derived from the exactly known energy as a function of the interaction strength with the help of the Hellmann-Feynman theorem (2.5). This theorem allows to calculate  $t(\nu)$  and  $v(\nu)$  separately from  $e(\nu)$  and gives — in addition to their normalizations (3.2) and (3.4) — exact relations for  $n_\kappa$  and the PD as shown in Equations (3.3) and (3.5) together with Equations (4.7) and (4.8), respectively. Equations (3.6) and (4.9) give additional exact integral relations between  $n_\kappa$  and the PD. We expect that similar relations can be derived for correlation function results [44, 45] based on the theory of Jack symmetric polynomials for values  $\nu = p/q$  with  $p$  and  $q$  relatively prime positive integers [34]. Thus an extension of our work to

these  $\nu$  is possible, albeit necessitating a different approach for the numerically stable evaluation of the products of integrals.

In summary, we have analyzed particle-number fluctuations and studied measures for the correlation strength based on the pair density and on the momentum distribution of the 1D quantum system of  $1/x_{ij}^2$  interacting particles. We made extensive use of the available exact solution and applied the Hellmann-Feynman theorem to the CS model. Our results show that further work is called for in order to make the qualitative terms ‘weak and strong correlation’ quantitatively precise presumably with a variety of quantities instead of a single index [13].

## Acknowledgments

RAR gratefully acknowledges support by the Deutsche Forschungsgemeinschaft (SFB393) and the hospitality of the Max-Planck-Institut für Physik komplexer Systeme (Dresden) for an extended stay where much of this work was started. PZ thanks the Max-Planck-Institut für Physik komplexer Systeme and P. Fulde for supporting this work.

## References

- [1] P. Fulde, *Electron Correlations in Molecules and Solids*, Springer, Berlin (1995).
- [2] F. Schautz, H.-J. Flad, and M. Dolg, *Theor. Chem. Acc.* **99**, 231 (1998) and references cited therein.
- [3] P. Ziesche, J. Tao, M. Seidl, and J. P. Perdew, *Int. J. Quantum Chem.* **77**, 819 (2000). Here it is shown how particle fluctuation is reduced by exchange in the ideal Fermi gas, and further reduced by Coulomb correlation in the interacting electron gas of 1, 2, or 3 dimensions.
- [4] S. Kurth and J. P. Perdew, *Int. J. Quantum Chem.* **77**, 814 (2000).
- [5] R. F. W. Bader, *Atoms in Molecules*, Clarendon, Oxford (1990).
- [6] C. Aslangul, R. Constanciel, R. Daudel, and Ph. Kottis, *Adv. Quantum Chem.* **6**, 93 (1972) and references cited therein.
- [7] J. F. Dobson, *J. Chem. Phys.* **94**, 4328 (1991).
- [8] J. Cioslowski and G. Liu, *J. Chem. Phys.* **110**, 1882 (1999) and references cited therein.
- [9] P.-O. Löwdin, *Phys. Rev.* **97**, 1474 (1955). Here it is asked for the meaning of  $\text{Tr}(\gamma - \gamma^2)$ , which is in our notation  $Nc(2)$ .
- [10] D. M. Collins, *Z. Naturforsch.* **48a**, 68 (1993); *Acta Cryst. A* **49**, 86 (1992).
- [11] C. J. Ramirez, J. H. M. Pérez, R. P. Sagar, R. O. Esquivel, M. Hô, and V. H. Smith, Jr., *Phys. Rev. A* **58**, 3507 (1998) and references cited therein.
- [12] P. Ziesche, O. Gunnarsson, W. John, and H. Beck, *Phys. Rev. B* **55**, 10270 (1997); P. Ziesche, V. H. Smith, Jr., M. Hô, S. P. Rudin, P. Gersdorf, and M. Taut, *J. Chem. Phys.* **110**, 6135 (1999); and references cited therein.
- [13] P. Ziesche, preprint mpi-pks/200001001 and *J. Mol. Structure (THEOCHEM)* **527**, 35 (2000).
- [14] B. Sutherland, *J. Math. Phys.* **12**, 246 (1971), B. Sutherland, *J. Math. Phys.* **12**, 251 (1971), B. Sutherland, *Phys. Rev. A* **4**, 2019 (1971), B. Sutherland, *Phys. Rev. A* **5**, 1372 (1972).
- [15] B. Sutherland, *Phys. Rev. B* **45**, 907 (1992), R. A. Römer and B. Sutherland, *Phys. Rev. B* **48**, 6058 (1993).
- [16] M. L. Mehta, *Random Matrices*, Academic Press, Boston, 1990.
- [17] F. Dyson, *J. Math. Phys.* **3**, 140 (1962).

- [18] A. Szabo and N. S. Ostlund, *Modern Quantum Chemistry*, Mc Graw-Hill, New York, 1982.
- [19] B. L. Hammond, W. A. Lester, Jr., P. J. Reynolds, *Monte Carlo Methods in Ab Initio Quantum Chemistry*, World Scientific, Singapore, 1994.
- [20] D.A. Mazziotti, Phys. Rev. A **60**, 4396 (1999); M. Ehara, Chem. Phys. Lett. **305**, 483 (1999); C. Valdemoro, L. M. Tel, and E. Pérez-Romero, Phys. Rev. A **61**, 032507 (2000).
- [21] P. Fulde, H. Stoll, and K. Kladko, Chem. Phys. Lett. **299**, 481 (1999).
- [22] A. M. Polyakov, Pis'ma Zh. Eksp. Teor. Fiz. **12**, 538 (1970), [JETP Lett. **12**, 381 (1970)].
- [23] A. A. Belavin, A. M. Polyakov, and A. B. Zamolodchikov, Nucl. Phys. B **241**, 333 (1984).
- [24] J. L. Cardy, Phys. Rev. Lett. **52**, 1575 (1984).
- [25] J. L. Cardy, in *Phase Transitions and Critical Phenomena*, edited by C. Domb and J. L. Lebowitz, Academic, New York, 1987, Vol. 11.
- [26] B. Sutherland and R. A. Römer, Phys. Rev. Lett. **71**, 2789 (1993).
- [27] B. Sutherland, R. A. Römer, and B. S. Shastry, Phys. Rev. Lett. **73**, 2154 (1994).
- [28] B. D. Simons and B. L. Altshuler, Phys. Rev. Lett. **70**, 4063 (1993).
- [29] B. D. Simons and B. L. Altshuler, Phys. Rev. B **48**, 5422 (1993).
- [30] V. E. Kravtsov and A. M. Tsvelik, (2000), cond-mat/0002120.
- [31] M. A. Olshanetsky and A. M. Perelomov, Phys. Rep. **71**, 313 (1981).
- [32] H. Hellmann, *Einführung in die Quantenchemie*, Deuticke, Leipzig, 1937, pp. 61, 285 (the original russian version is of 23 October 1936: G. Gel'man, Quantenchemie, ONTI, Moscow and Leningrad, p. 428); R. P. Feynman, Phys. Rev. **56**, 340 (1939); what usually is referred to as Hellmann-Feynman theorem has been first formulated by P. Güttinger, Z. Phys. **73**, 169 (1932), see his Eq. (11). This result is implicitly contained in Eq. (28) of M. Born and V. Fock, Z. Phys. **51**, 165 (1928). Whereas in these papers any parameter is considered, Hellmann and later Feynman explicitly referred to the special case of nuclear coordinates within the Born-Oppenheimer approximation, leading to the 'Hellmann-Feynman' forces upon nuclei. Within perturbation theory the theorem was already given by E. Schrödinger, Ann. Phys. (Leipzig) [4], **80**, 437 (1926). Thus the theorem is due to Schrödinger, Born, Fock, Güttinger, Hellmann, and Feynman.
- [33] L. D. Landau and E. M. Lifshitz, *Quantum Mechanics*, Pergamon, Oxford, 1977, §35.
- [34] Z. N. C. Ha, *Quantum Many-Body Systems in One Dimension*, World Scientific, Singapore (1996).
- [35] We emphasize that the replacement  $\mu/x_{ij}^2 \rightarrow \mu/[L \sin(\pi x_{ij}/L)/\pi]^2$  is used for periodic systems as discussed in [14, 15].
- [36] F. D. M. Haldane, J. Phys. C: Solid State Phys. **14**, 2585 (1981).
- [37] H. J. Schulz, G. Cuniberti, P. Pieri, cond-mat/9807366.
- [38] N. Kawakami and S.-K. Yang, Phys. Rev. Lett. **67**, 2493 (1991).
- [39] H. Yokoyama and M. Ogata, Phys. Rev. Lett. **67**, 3610 (1991).
- [40] Y. Takada and H. Yasuhara, Phys. Rev. B **44**, 7879 (1991).
- [41] F. Gebhardt and D. Vollhardt, Phys. Rev. Lett. **59**, 1472 (1987).
- [42] B. S. Shastry, Phys. Rev. Lett. **60**, 639 (1988).
- [43] F. D. M. Haldane, Phys. Rev. Lett. **60**, 635 (1988).
- [44] Z. N. C. Ha, Phys. Rev. Lett. **73**, 1574 (1994); F. Lesage, V. Pasquier, and D. Serban, Nuc. Phys. B **435**, 585 (1995).
- [45] P. J. Forrester, Mod. Phys. Lett. B **9**, 359 (1995).
- [46] H. Yasuhara and Y. Kawazoe, Physica **85A**, 416 (1976).
- [47] T. Kato, Commun. Pure Appl. Math. **10**, 151 (1957); see also R. T. Pack and W. B. Brown, J. Chem. Phys. **45**, 556 (1966) and S. Y. Chang, E. R. Davidson, and G. Vincow, J. Chem. Phys. **52**, 1740 (1970).
- [48] J.C. Kimball, J. Phys. A **8**, 1513 (1975), see also Refs. [40, 46].

**Table 1.** On-top exponent and coefficients of the PD according to Equation (4.1).

$\nu$	0	1/2	3/2
$\alpha$	1	2	4
$A$	$\frac{\pi}{6}$	$\frac{1}{3}$	$\frac{16}{135}$
$a_1$	0	0	0
$a_2$	$-\frac{1}{10}$	$-\frac{2}{15}$	$-\frac{8}{35}$
$a_3$	$\frac{2}{45\pi}$	0	0
$a_4$	$\frac{1}{280}$	$\frac{1}{105}$	$\frac{32}{1225}$
$a_5$	$-\frac{4}{1575\pi}$	0	0
$a_6$	$-\frac{1}{15120}$	$-\frac{2}{4725}$	$-\frac{2176}{1091475}$
$a_7$	$\frac{4}{55125\pi}$	0	0
$a_8$	$\frac{1}{1330560}$	$\frac{2}{155925}$	$\frac{125696}{1092566475}$

**Table 2.** Dimensionless cumulant PD  $h(y)$  and the structure factor  $S(q)$  used for the computation of  $\Delta N_X$  and  $\Sigma_1(\nu)$  as in Equations (5.2) and (5.4).

$\nu$	$h(y)$	$S(q) = 1 - \tilde{h}(q)/\pi$
0	$\left(\frac{\sin y}{y}\right)^2 - \left[\text{Si}(y) - \frac{\pi}{2}\right] \frac{d}{dy} \frac{\sin y}{y}$	$\left[q - \frac{q}{2} \ln(1+q)\right] \theta(2-q)$ $+ \left[2 - \frac{q}{2} \ln \frac{q+1}{q-1}\right] \theta(q-2)$
$\frac{1}{2}$	$\left(\frac{\sin y}{y}\right)^2$	$\frac{q}{2} \theta(2-q) + \theta(q-2)$
$\frac{3}{2}$	$\left(\frac{\sin 2y}{2y}\right)^2 - \text{Si}(2y) \frac{d}{d2y} \frac{\sin 2y}{2y}$	$\left[\frac{q}{4} - \frac{q}{8} \ln  1 - \frac{q}{2} \right] \theta(4-q)$ $+ \theta(q-4)$

**Table 3.** Coefficients as in Equation (4.3a) – Equation (4.3c) calculated from the numerically determined momentum distribution  $n_\kappa$  for  $\nu = 0$  and  $3/2$  (at  $n = 1/2L_0$ ).

$\nu = 0$			
$\kappa \in [0, 1]$		$\kappa \in [1, 2]$	$\kappa \in [2, \infty]$
$B$	0.863355	$B$	0.863355
$b_1^-$	-0.746775	$b_1^+$	-0.750439
$b_2^-$	0.731357	$b_2^+$	0.747380
$b_3^-$	-0.420828	$b_3^+$	-0.433779
		$b_4^+$	0.009552

$\nu = 3/2$			
$\kappa \in [0, 1]$		$\kappa \in [1, 2]$	$\kappa \in [2, \infty]$
$B$	0.552286	$B$	0.552286
$b_1^-$	0.434380	$b_1^+$	1.467126
$b_2^-$	-0.570516	$b_2^+$	-4.156361
		$b_3^+$	4.180551
		$b_4^+$	-1.606130

**Table 4.** Coefficients of the small- $X$  expansion of  $\frac{(\Delta N_X)^2}{N_X}$  as in Equation (5.3).

$\nu$	0	1/2	3/2
$d_1$	-1	-1	-1
$d_2$	$\frac{\pi^2}{18}$	0	0
$d_3$	0	$\frac{\pi^2}{18}$	0
$d_4$	$-\frac{\pi^4}{600}$	0	0
$d_5$	0	$-\frac{2\pi^4}{675}$	$\frac{16\pi^4}{2025}$

## Appendix A. Certain integrals

The following identities are valid with  $\text{Si}(x) = \int_0^x dy[\sin(y)/y]$ :

$$\int_0^\infty \frac{dx}{\pi} \frac{\sin x}{x} = \frac{\text{Si}(\infty)}{\pi} = \frac{1}{2} , \quad (\text{A.1})$$

$$\int_0^\infty \frac{dx}{\pi} \left( \frac{\sin x}{x} \right)^2 = \frac{1}{2} , \quad (\text{A.2})$$

$$\int_0^\infty \frac{dx}{\pi} [\text{Si}(\infty) - \text{Si}(x)] \frac{d}{dx} \frac{\sin x}{x} = 0 , \quad (\text{A.3})$$

$$\int_0^\infty \frac{dx}{\pi} \text{Si}(x) \frac{d}{dx} \frac{\sin x}{x} = -\frac{1}{2} , \quad (\text{A.4})$$

$$\int_0^\infty \frac{dx}{\pi} \frac{1}{x^2} \left[ 1 - \left( \frac{\sin x}{x} \right)^2 \right] = \frac{1}{3} , \quad (\text{A.5})$$

$$\int_0^\infty \frac{dx}{\pi} \frac{1}{x^2} \text{Si}(x) \frac{d}{dx} \frac{\sin x}{x} = -\frac{2}{9} . \quad (\text{A.6})$$

Equations (A.2) – (A.4) determine the normalization of the PD's (4.10) – (4.12). Equations (A.5) and (A.6) determine the interaction energy  $v$  for the HF approximation and for  $\nu = 3/2$ . For the fluctuation analysis with Equations (5.1) and (5.2)

$$\frac{2}{\pi} \int_0^\infty dy \cos(qy) \left( \frac{\sin y}{y} \right)^2 = \left( 1 - \frac{q}{2} \right) \theta(2 - q) , \quad (\text{A.7})$$

$$\frac{2}{\pi} \int_0^\infty dy \sin(qy) \text{Si}(y) \frac{\sin y}{y} = -\frac{1}{2} \ln |1 - q| \theta(2 - q) , \quad (\text{A.8})$$

$$\frac{2}{\pi} \int_0^\infty dy \cos(qy) \text{Si}(y) \frac{d}{dy} \frac{\sin y}{y} = -\left[ 1 - \frac{q}{2} + \frac{q}{2} \ln |1 - q| \right] \theta(2 - q) , \quad (\text{A.9})$$

$$\int_0^\infty dy \cos(qy) \frac{d}{dy} \frac{\sin y}{y} = -\left[ 1 - \frac{q}{2} \ln \left| \frac{1+q}{1-q} \right| \right] , \quad (\text{A.10})$$

$$\frac{2}{\pi} \int_0^\infty dy \cos(qy) \frac{\sin y}{y} \frac{d^2}{dy^2} \frac{\sin y}{y} = \frac{1}{6} (q-2) (q^2 - q + 1) \theta(2 - q) , \quad (\text{A.11})$$

$$2\pi \int_0^Y dy_1 \int_0^Y dy_2 \left( \frac{\sin |y_1 - y_2|}{|y_1 - y_2|} \right)^2 =$$

$$2 \int_0^2 dq \frac{1 - \cos qY}{q^2} (1 - \frac{q}{2}) =$$

$$1 - \cos 2Y - 2Y \text{Si}(2Y) + \int_0^{2Y} dz \frac{1 - \cos z}{z} . \quad (\text{A.12})$$

## Appendix B. Kimball like theorems for $n(x_{12})$ and $n_\kappa$

The small separation or on-top behavior of the PD  $n(x_{12})$  is derived here similarly as Kato [47] and Kimball [48] found the cusp relation  $dg(k_F r)/dr|_{r=0} = g(0)/a_B$  [or  $g'(0) = \alpha r_s g(0)$ ,  $\alpha = (4/9\pi)^{1/3}$ ] for the pair correlation of the 3D uniform electron gas. Let us consider two adjacent electrons with the center-of-mass and relative coordinates,  $X = (x_1 + x_2)/2$  and  $x = x_1 - x_2$ , respectively. Focusing on the  $x$  dependence the Schrödinger equation can be written as

$$\left[ -\frac{d^2}{dx^2} + \frac{\lambda(\lambda-1)}{x^2} \right] \varphi(x) \tilde{\Phi}(X, x_3, \dots) = (E - H') \varphi(x) \tilde{\Phi}(X, x_3, \dots), \quad (\text{B.1})$$

where  $H'$  contains the remaining terms in the Hamiltonian. Because  $E - H'$  is non-singular as  $x$  approaches zero, it is unimportant for small  $x$ . To lowest order in  $x$  we therefore have  $\varphi(x) = x^\lambda + \dots$ , from which immediately follows  $n(x) \sim x^{2\lambda}$  for the PD, see Equation (4.1). This can be concluded for  $\lambda \neq 1$  also directly from the many-body wave function  $\Phi \sim \prod_{i < j} x_{ij}^\lambda$  [14] and for  $\lambda = 1$  from Equation (4.11).

A similar treatment of the asymptotic large  $\kappa$  behavior of the momentum distribution  $n_\kappa$  seems to lead in Equation (4.3c) to the conclusion  $\gamma = 2\lambda + 2$ . This corresponds to  $n_{\kappa \rightarrow \infty} \sim g(0)/\kappa^8$  for the 3D uniform electron gas [40, 46, 48].

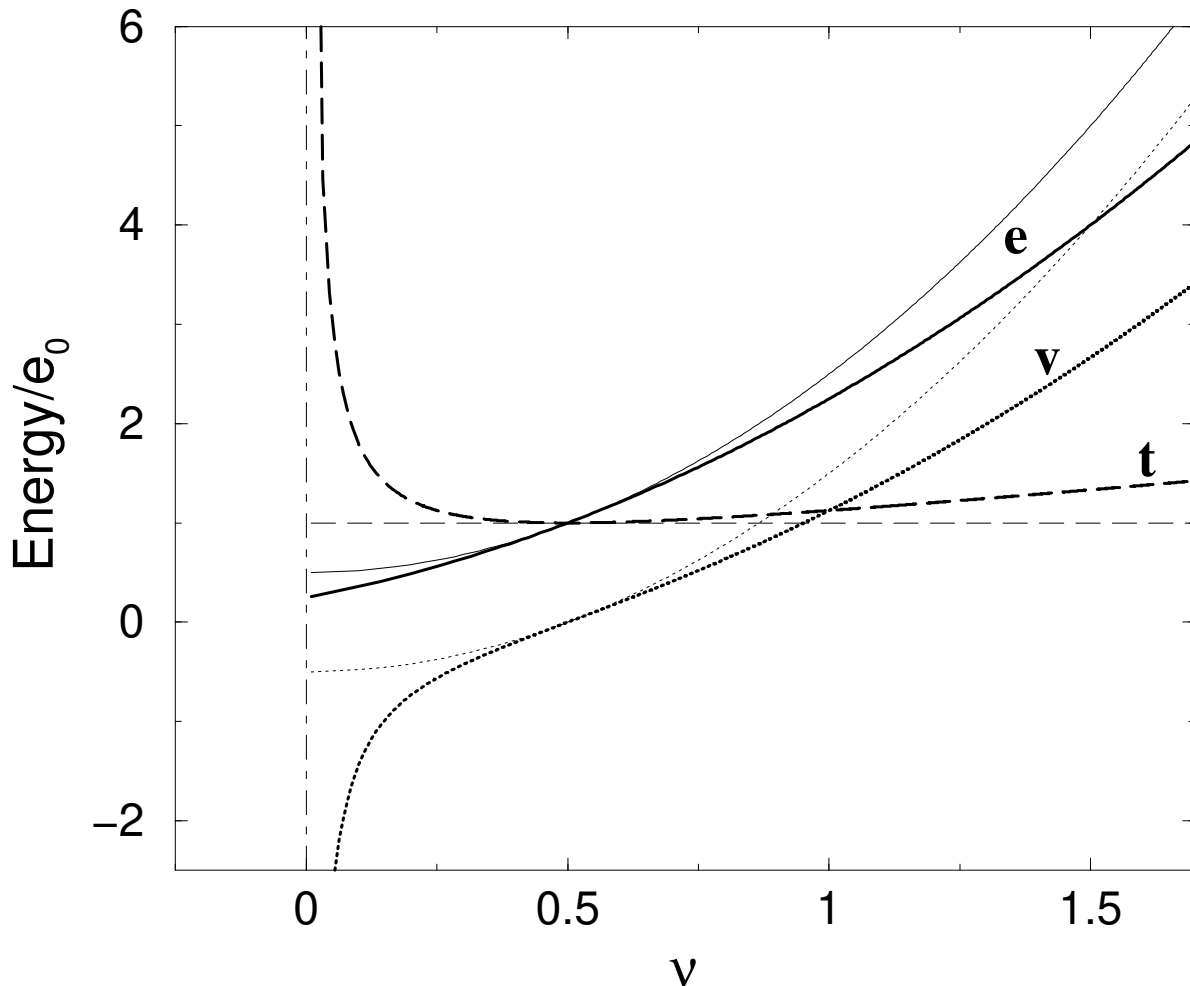


**Figure 1.** Bulk energy  $e$  (solid), kinetic energy  $t$  (dashed), and potential energy  $v$  (dotted) plotted as functions of interaction strength parameter  $\nu$ . Thin lines denote the results of the Hartree-Fock approximation, thick lines are exact. The thin dashed-dotted line indicates the “fall-into-the-origin” at  $\nu = 0$ .

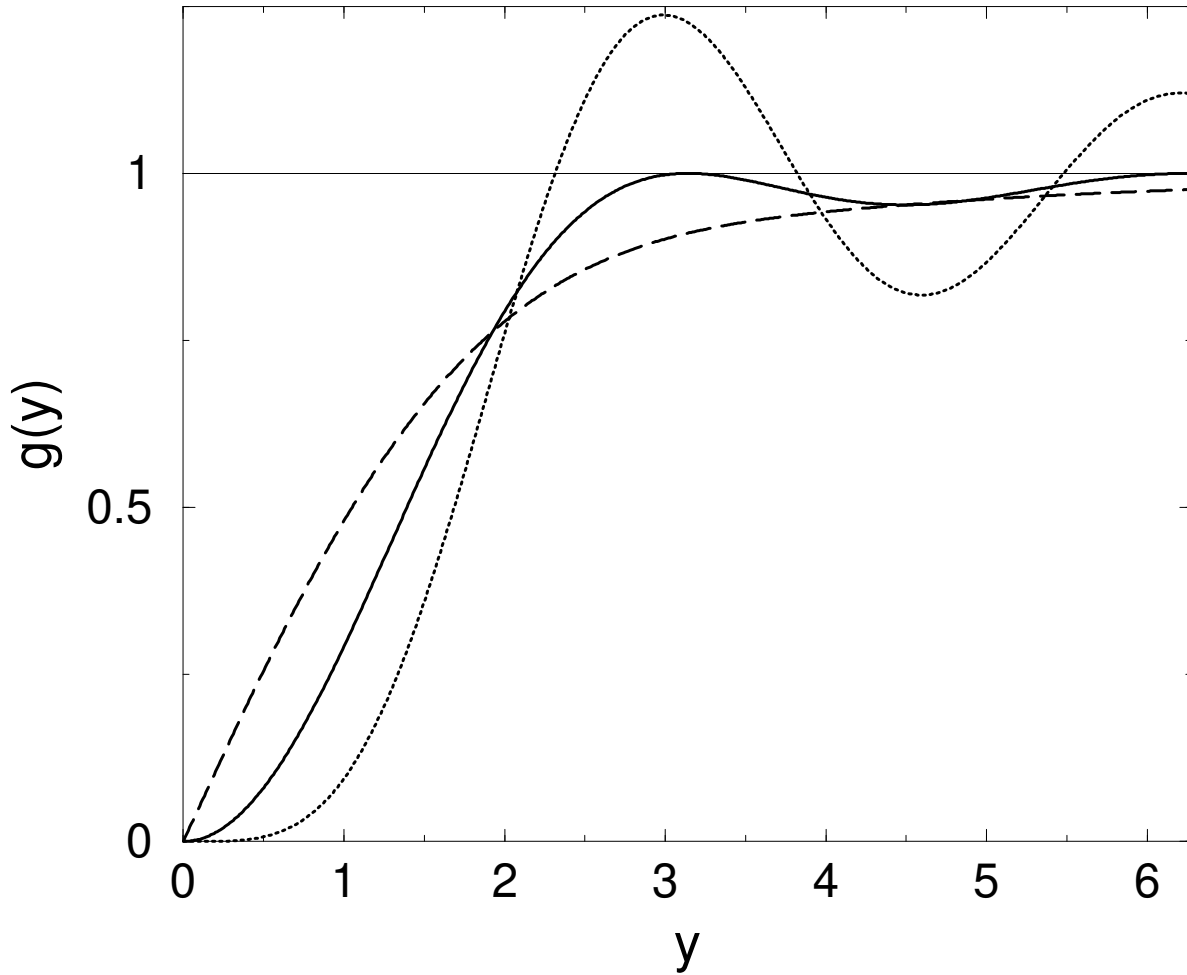


**Figure 2.** Dimensionless PD  $g(y) = n(x_{12})/n^2$  as a function of the dimensionless inter-particle separation  $y = k_F x_{12}$  for  $\nu = 0$  (dashed),  $1/2$  (solid), and  $3/2$  (dotted). The thin line is a guide to the eye only.

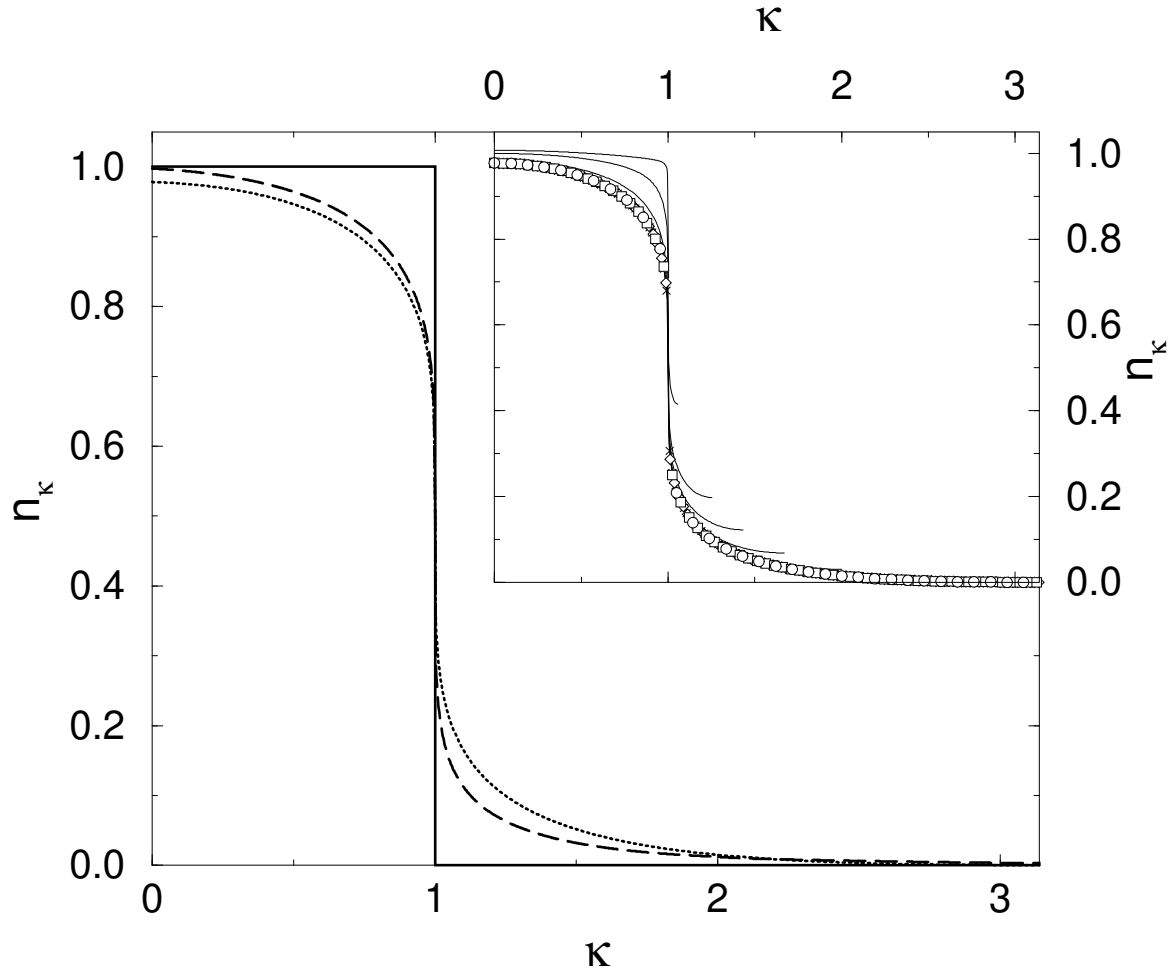


**Figure 3.** Fermionic momentum distributions  $n_\kappa$  vs.  $\kappa = k/k_F$  with  $\nu = 0$  (dashed),  $1/2$  (solid), and  $3/2$  (dotted). Inset:  $n_\kappa$  for  $\nu = 3/2$  and  $L = 401$  computed with  $N = 21, 41, 81, 121, 161, 201, 241, 281, 321, 361$ , and  $401$ . The data for  $N = 21(\circ)$ ,  $41(\square)$ ,  $81(\diamond)$ , and  $121(\times)$  do not show any density dependence whereas the larger density data (lines) do.

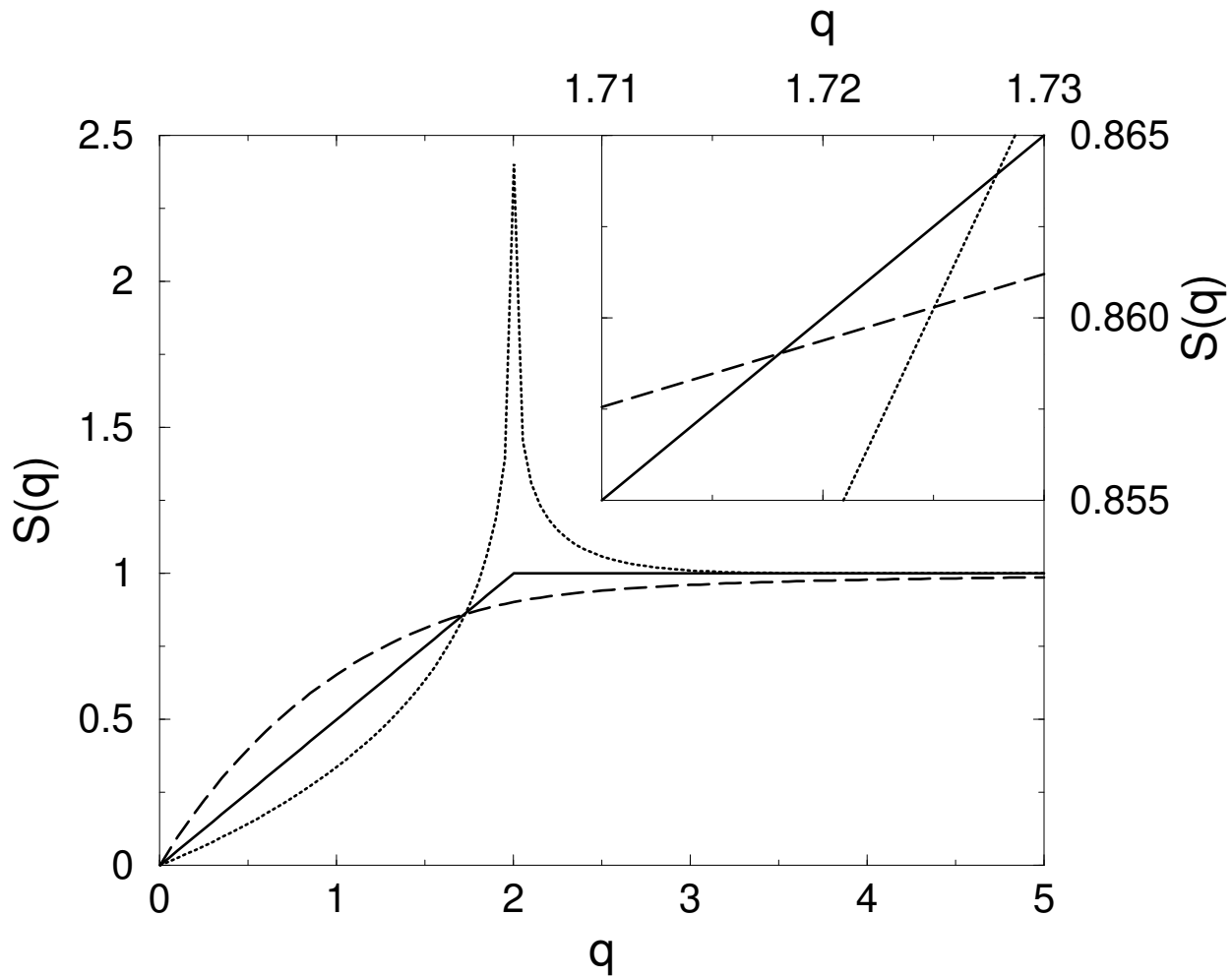


**Figure 4.** Static structure factor  $S(q) = 1 - \tilde{h}(q)/\pi$  for  $\nu = 0$  (dashed),  $1/2$  (solid), and  $3/2$  (dotted). Inset: The three curves do not coincide at a single point close to  $q \approx 1.72$ .

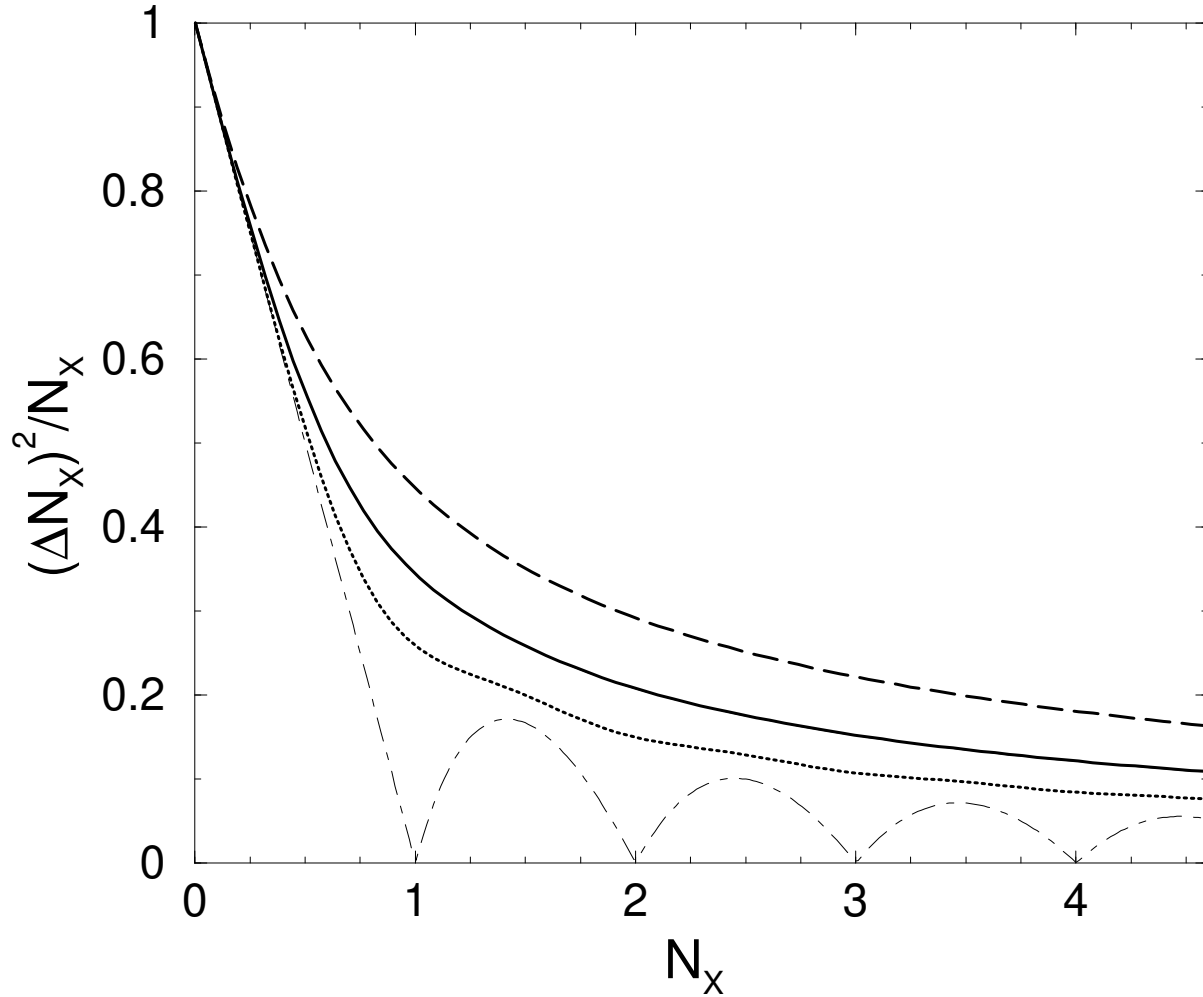


**Figure 5.** Particle-number fluctuation  $(\Delta N_X)^2 / N_X$  in domains  $X$  of the CS model after Equation (5.2) for  $\nu = 0$  (dashed),  $1/2$  (solid), and  $3/2$  (dotted). The dashed-dotted line corresponds to  $(\Delta N_X)^2 / N_X$  for strict correlation. [3]

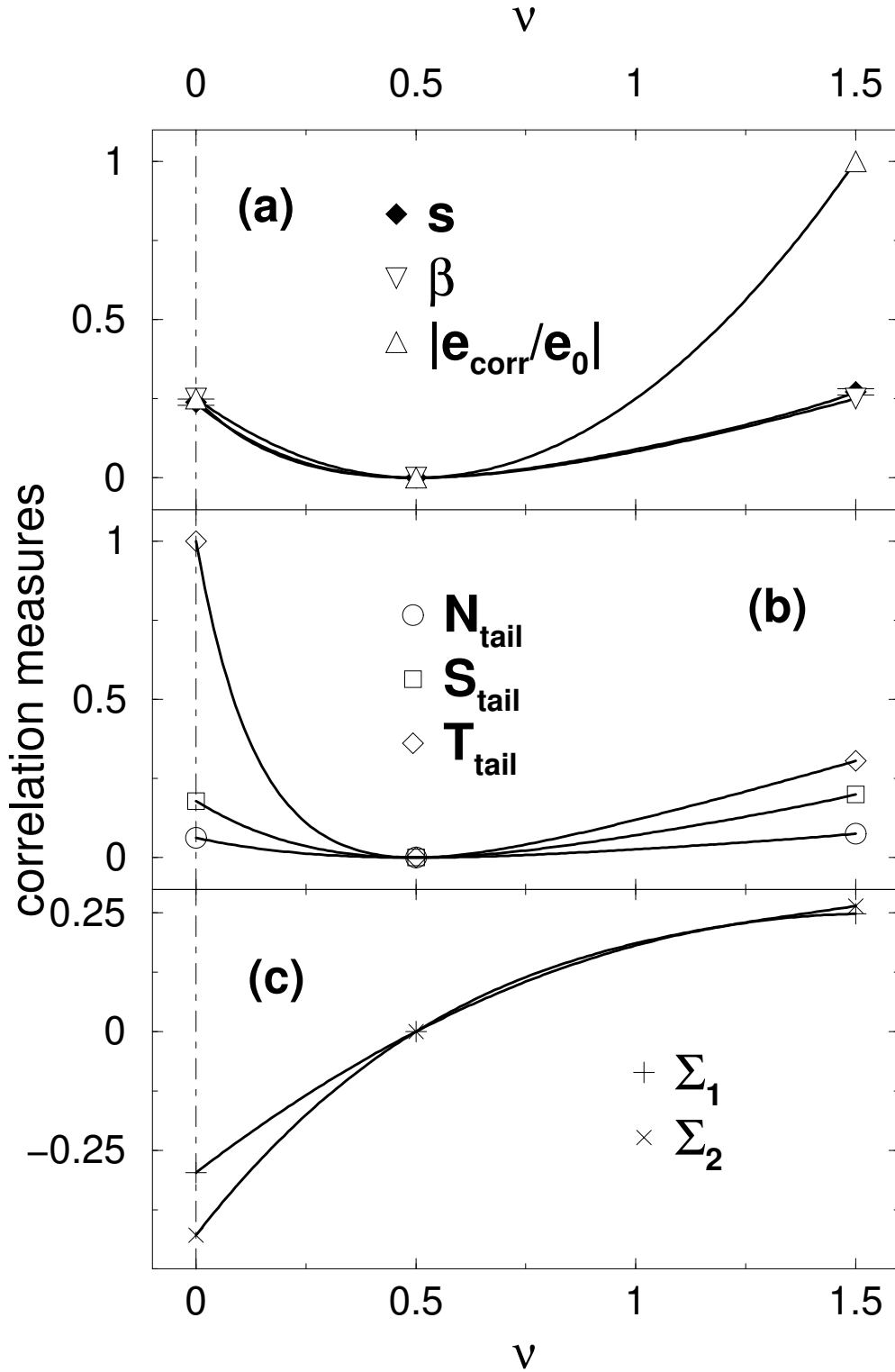


**Figure 6.** Correlation measures based on (a) the bulk of the momentum distribution, (b) the tail of the momentum distribution, and (c) the PD shown as functions of  $\nu$ . The solid lines are guides to the eye only. The thin dashed-dotted line indicates the “fall-into-the-origin” at  $\nu = 0$ .

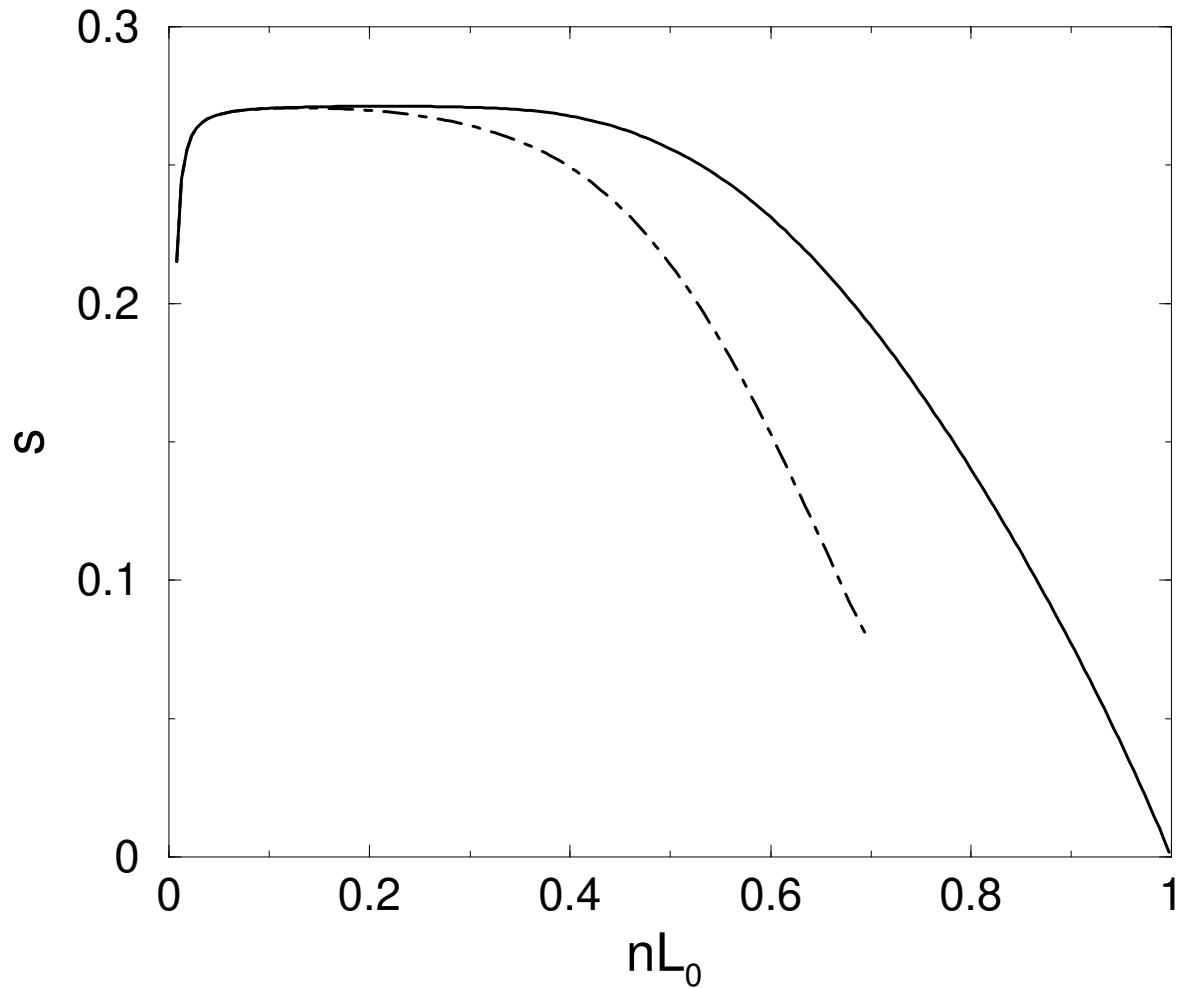


**Figure 7.** Correlation entropy (5.6) for Fermions (solid line) as a function of density at  $\nu = 3/2$ . The dashed-dotted line corresponds to  $s$  obtained for the discrete CS model.

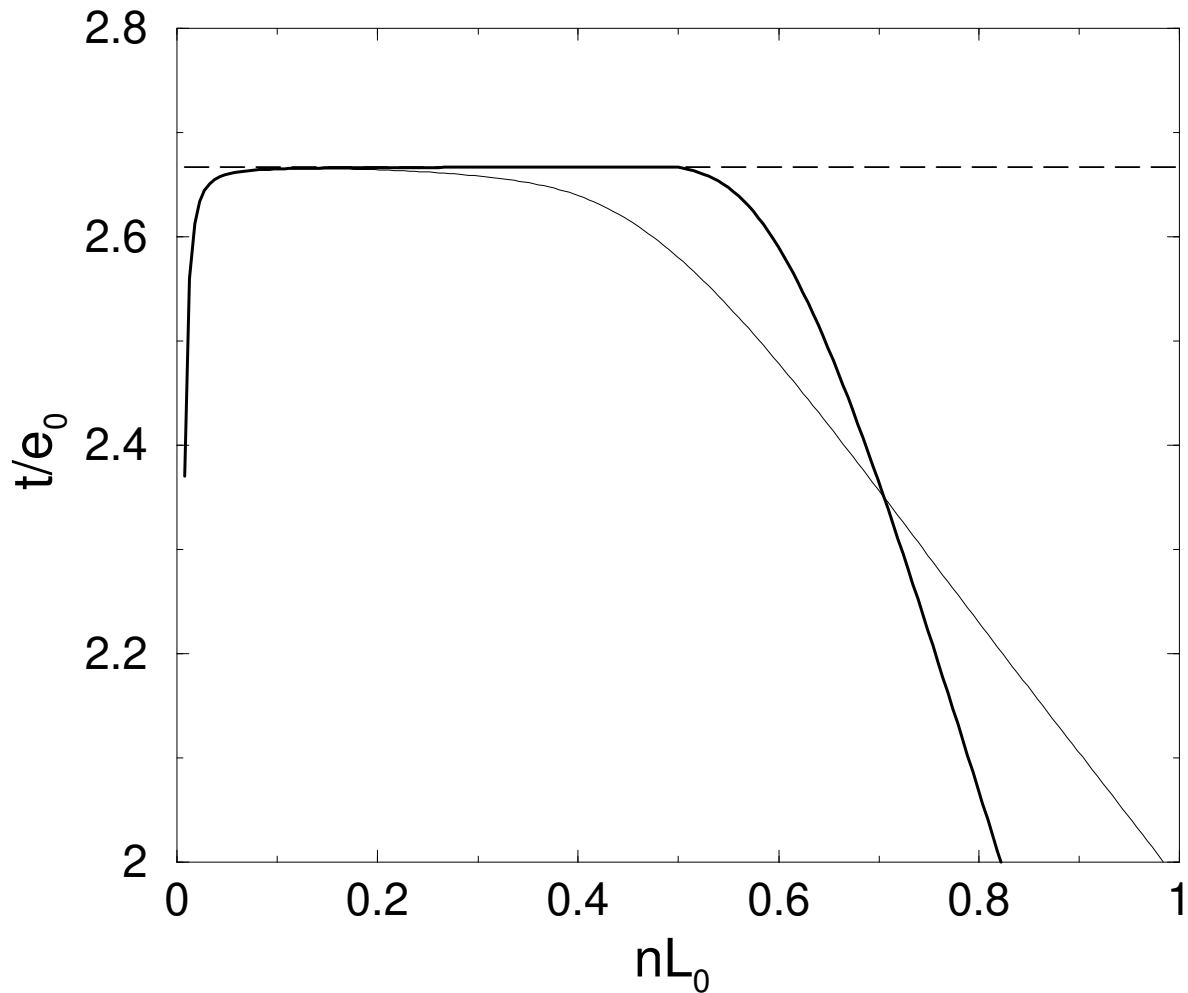


**Figure 8.** Kinetic energy  $t$  as computed from the Hellman-Feynman theorem (2.5) (dashed line), and  $t$  from Equation (2.6) (solid lines) for Fermions (thick line) and Bosons (thin line) as a function of density at  $\nu = 3/2$ .

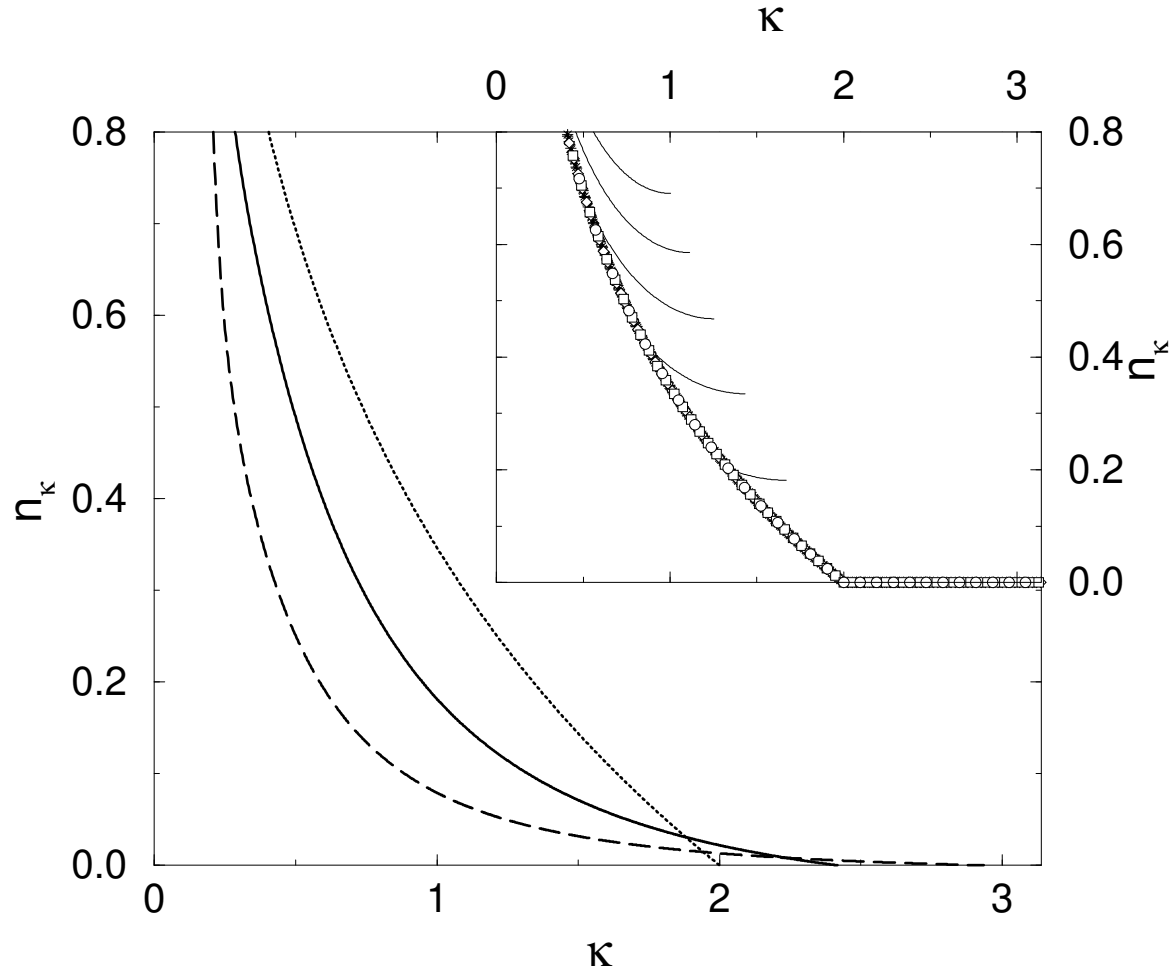


**Figure 9.** Bosonic momentum distributions  $n_\kappa$  vs.  $\kappa = k/k_F$  with  $\nu = 0$  (dashed),  $1/2$  (solid), and  $3/2$  (dotted). Inset:  $n_\kappa$  for  $\nu = 3/2$ ,  $L = 401$  and particle numbers identical to the inset of Figure 3. The data for  $N = 21(\circ)$ ,  $41(\square)$ ,  $81(\diamond)$ ,  $121(\times)$ ,  $161(+)$ , and  $201(*)$  do not show any density-dependence effects.